Multi-Ion Distributions in the Cytoplasmic Domain of Inward Rectifier Potassium Channels

J. L. Robertson,[†‡] L. G. Palmer,[‡] and B. Roux[†]

[†]Department of Biochemistry and Molecular Biology, University of Chicago, Chicago, Illinois; and
[‡]Department of Physiology and Biophysics, Weill Cornell Medical College, New York, New York

SUPPORTING INFORMATION - Robertson J. L. et al.

TABLE S1

Channel	Model	Ions	Q_{prot}	Vol ($Å^3$)	N_K	N_{Cl}	N_{water}	Time (ns)
Kir1.1/ROMK	1	KCl	+20	807131	486	506	26011	12
	2			848051	510	530	27332	19
	3			807280	486	506	26016	17
Kir2.1/IRK	1	KCl	-24	811992	512	488	26166	13
	2			804171	508	484	25912	15
	3			810837	512	488	26127	13
Kir1.1/ROMK	1	4 Mg^{2+} + KCl	+20	807130	485	513	26003	20
	2			848051	510	538	27324	21
	3			807280	486	514	26008	20
Kir2.1/IRK	1	4 Mg^{2+} + KCl	-24	811992	504	488	25912	19
	2			804171	500	484	25913	18
	3			810837	504	488	26135	29
Kir1.1/ROMK	1	1 SPM^{4+} + KCl	+20	807131	485	509	25983	19
	2			848051	510	534	27328	19
	3			807280	486	514	26008	20
Kir2.1/IRK	1	1 SPM^{4+} + KCl	-24	811992	508	488	26144	18
	2			804171	504	484	25916	19
	3			810837	508	488	26131	18
Kir1.1/ROMK	1	2 SPM^{4+} + KCl	+20	807130	481	509	25956	10
Kir2.1/IRK	1	2 SPM^{4+} + KCl	-24	811992	504	488	26125	10
Kir2.1/IRK	1U4F	KCl	-28	943580	596	568	30404	15

Table S1. Molecular dynamics simulation parameters. The volume is calculated as the number of water molecules before ion replacement * 29.89 A^3. N_{water} represents the final number of water molecules after addition of ions.

TABLE S2

PDB	Homologue	Species	Resolution	Structural details
1N9P[1]	Kir3.1/GIRK1	*Mus musculus*	1.80 Å	Isolated cytoplasmic domain with open G-loop gate.
1P7B[2]	KirBac1.1	*Burkholderia pseudomallei*	3.65 Å	Full-length channel with closed helix-bundle gate and closed G-loop gate.
1U4E[3]	Kir3.1/GIRK1	*Mus musculus*	2.09 Å	Isolated cytoplasmic domain with open G-loop gate
1U4F[3]	Kir2.1/IRK1	*Mus musculus*	2.41 Å	Isolated cytoplasmic domain with closed pore.
1XL4[4]	KirBac3.1	*Magnetospirillum magnetotacticum*	2.60 Å	Full-length channel with closed helix-bundle gate and open G-loop gate, possible Mg^{2+} in selectivity filter .
1XL6[4]	KirBac3.1		2.85 Å	Full-length channel with closed helix-bundle gate and open G-loop gate, possible $Spermine^{4+}$ in pore.
2GIX[3]	Kir2.1/IRK1 + R218Q/T309K	*Mus musculus*	2.02 Å	Isolated cytoplasmic domain with closed G-loop gate and one ion density at the cytoplasmic entrance.
2QKS[5]	Prokaryotic Kir - Kir3.1/GIRK1 chimera	*Burkholderia xenovorans* – *Mus musculus*	2.20Å	Full-length channel with two conformations in the unit cell: (i) helix-bundle gate closed and G-loop gate open, and (ii) helix-bundle gate intermediately open and G-loop gate closed. In (i), two ion densities are observed near the G-loop.
2WLH[4]	KirBac3.1	*Magnetospirillum magnetotacticum*	3.28 Å	Full-length channel with closed helix-bundle gate and open G-loop gate.
2WLI[4]	KirBac3.1		3.09 Å	Full-length channel with intermediately open helix-bundle gate and open G-loop gate.
2WLJ[4]	KirBac3.1		2.60 Å	Re-refinement of 1XL4, possible Mg^{2+} in selectivity filter and $Spermine^{4+}$ in cytoplasmic domain
2WLK[4]	KirBac3.1		2.80 Å	Re-refinement of 1XL6, possible $Spermine^{4+}$ in pore
2WLL[4]	KirBac1.1	*Burkholderia pseudomallei*	3.65 Å	Re-refinement of 1P7B, possible Mg^{2+} in selectivity filter
2WLM[4]	KirBac3.1	*Magnetospirillum magnetotacticum*	3.61 Å	Full-length channel with closed helix-bundle gate and open G-loop gate.
2WLN[4]	KirBac3.1		3.44 Å	Full-length channel with closed helix-bundle gate and open G-loop gate.
2WLO[4]	KirBac3.1		4.04 Å	Full-length channel with intermediately open helix-bundle gate and open G-loop gate.
2X6A[4]	KirBac3.1 + Q170A		3.10 Å	Full-length channel with closed helix-bundle gate and open G-loop gate.
2X6B[4]	KirBac3.1 +		3.30 Å	Full-length channel with closed helix-

	Q170A			bundle gate and open G-loop gate. Anomalous Ba^{2+} signal in selectivity filter
2X6C[4]	KirBac3.1 + Q170A		2.70 Å	Full-length channel with closed helix-bundle gate and open G-loop gate. Anomalous Sm^{3+} signal in cytoplasmic domain.
3JYC[6]	Kir2.2/IRK2	*Gallus gallus*	3.1 Å	Full-length channel with closed helix-bundle gate and intermediately opene G-loop gate.
3K6N[7]	Kir3.1/GIRK1 + S225E	*Mus musculus*	2.0 Å	Isolated cytoplamic domain with open G-loop gate. Five ion densities observed inside the pore.
3SPC[8]	Kir2.2/IRK2 + PPA (PIP_2 head-group)	*Gallus gallus*	2.45 Å	Full-length channel with closed helix-bundle gate and intermediately open G-loop gate.
3SPG[8]	Kir2.2/IRK2 + R186A + PIP_2		2.61 Å	Full-length channel with closed helix-bundle gate and closed G-loop gate.
3SPH[8]	Kir2.2/IRK2 + I223L + PIP_2		3.00 Å	Full-length channel with closed helix-bundle gate and closed G-loop gate.
3SPI[8]	Kir2.2/IRK2 + PIP_2 (short chain analog)		3.31 Å	Full-length channel with closed helix-bundle gate and closed G-loop gate.
3SPJ[8]	Kir2.2/IRK2 + I223L		3.31 Å	Full-length channel with closed helix-bundle gate and closed G-loop gate.
3SYA[9]	Kir3.2/GIRK2 + PIP_2	*Mus musculus*	2.98 Å	Full-length channel with intermediately open helix-bundle gate and closed G-loop gate.
3SYC[9]	Kir3.2/GIRK2 + D228N		3.41 Å	Full-length channel with closed helix-bundle gate and closed G-loop gate.
3SYO[9]	Kir3.2/GIRK2		3.54 Å	Full-length channel with intermediately open helix-bundle gate and closed G-loop gate.
3SYP[9]	Kir3.2/GIRK2 + R201A		3.12 Å	Full-length channel with closed helix-bundle gate and open G-loop gate.
3SYQ[9]	Kir3.2/GIRK2 + R201A + PIP_2		3.44 Å	Full-length channel with two opposing subunits in different conformations: (i) intermediately open helix-bundle gate and open G-loop gate, and (ii) intermediately open helix-bundle and closed G-loop gate.

Table S2. Comparison of x-ray crystal structures of Kir channels. Structures are listed according to date of entry into the PDB. For the the conformation of the gates, open describes a pore radii greater than 6 Å, intermediately-open 3-5 Å, and closed < 3 Å, based on radii calculations in Supplementary Figures 2-5.

TABLE S3

	Kir Bac 1.1 (1P7B*)	Kir Bac 1.1 (open model)	Kir3.1 GIRK1 (1N9P)	Kir2.1 IRK1 (1U4F)	Kir Bac 3.1 (2WLI)	Kir2.2 IRK (3JYC)	Kir3.2 GIRK2 (3SYQ open model)	Kir1.1 ROMK1 (open model)	Kir2.1 IRK1 (open model)
KirBac 1.1 (1P7B*)		1.9 Å	3.1 Å	3.2 Å	3.0 Å	3.3 Å	3.2 Å	2.4 Å	2.5 Å
KirBac 1.1 (open model)			3.3 Å	3.5 Å	3.4 Å	3.5 Å	3.7 Å	1.8 Å	2.0 Å
Kir3.1 GIRK1 (1N9P)				1.6 Å	2.8 Å	1.8 Å	1.6 Å	3.7 Å	3.8 Å
Kir2.1 IRK1 (1U4F)					2.8 Å	0.8 Å	1.2 Å	3.8 Å	3.9 Å
KirBac 3.1 (2WLI)						2.8 Å	2.7 Å	3.7 Å	3.7 Å
Kir2.2 IRK (3JYC)							1.5 Å	3.8 Å	3.9 Å
Kir3.2 GIRK2 (3SYQ open model)								3.9 Å	3.9 Å
Kir1.1 ROMK1 (open model #1)									1.6 Å
Kir2.1 IRK1 (open model #1)									

Table S3. RMSD of Cα atoms of a single subunit of cytoplasmic domain crystal structures and models. Regions containing insertions or deletions were removed from the alignment. Residues were aligned using the RMSD calulator in VMD. (*) For 1P7B, missing loops were built based on homology with the Kir3.1/GIRK structure 1N9P prior to alignment.

FIG. S1

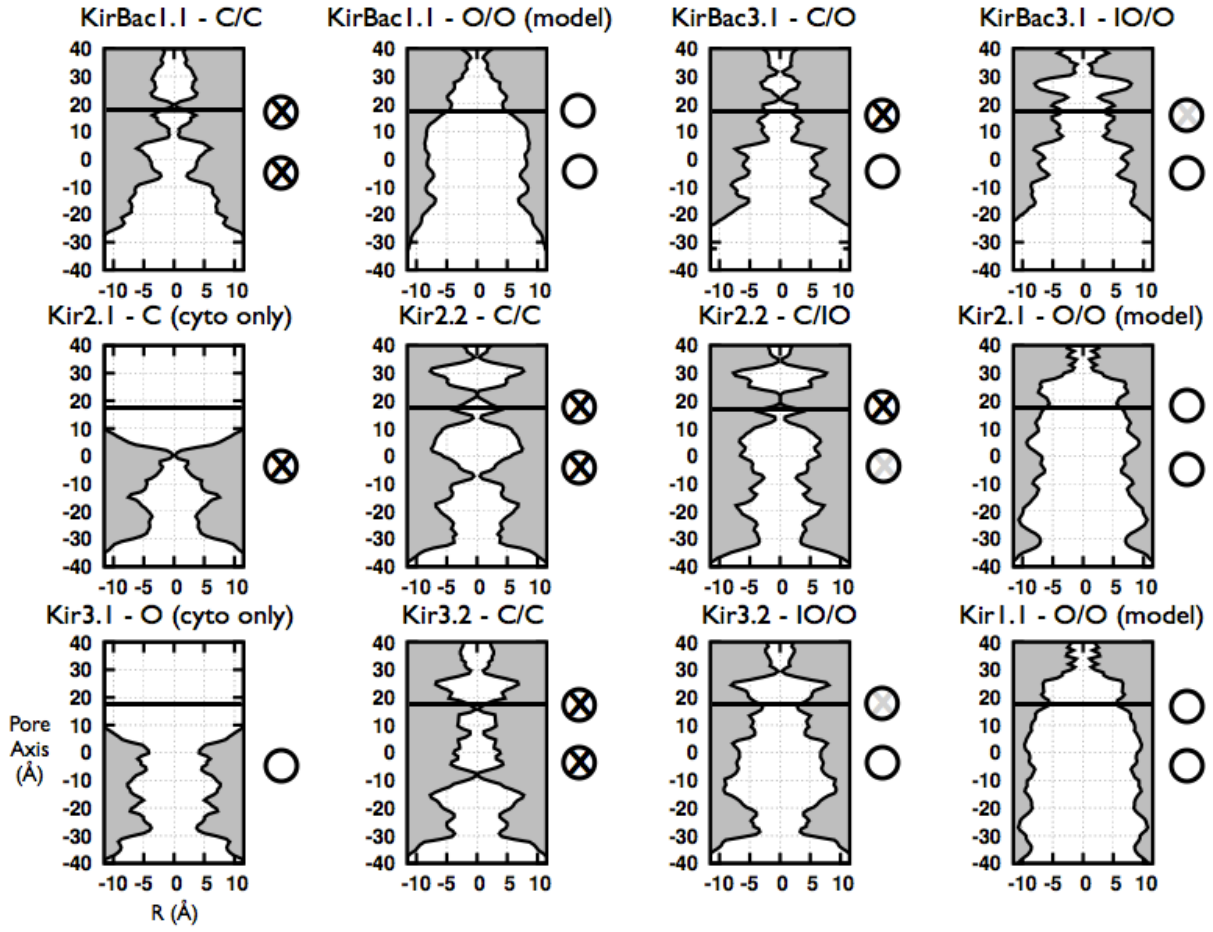

Figure S1. Calculated pore radius profiles for Kir crystals structures and homology models. For each, the structure was aligned onto the Z-axis, referred to as the Pore Axis (Å). The solid black line designates the lower membrane interface, where the helix-bundle gate is positioned. The G-loop gate is positioned at 0 Å. The gates are described as closed (C-blocked circle), open (O-open circle) and intermediate open (IO-grey blocked circle). KirBac1.1 – C/C (1P7B with loops built from 1N9P), KirBac1.1 – O/O (model based on KirBac3.1 electron crystallography density map), KirBac3.1 – C/O (2WLH), KirBac3.1 – IO/O (2WLI), Kir2.1 – C (cytoplasmic domain only 1U4F), Kir2.2 – C/C (3SPJ), Kir2.2 – C/IO (3JYC), Kir2.1 – O/O (model), Kir3.1 – O (cytoplasmic domain only 1N9P), Kir3.2 – C/C (3SYC), Kir3.2 – IO/O (3SYQ, open model), Kir1.1 – O/O (model). Radii are calculated according to previously described methods (10).

FIG. S2

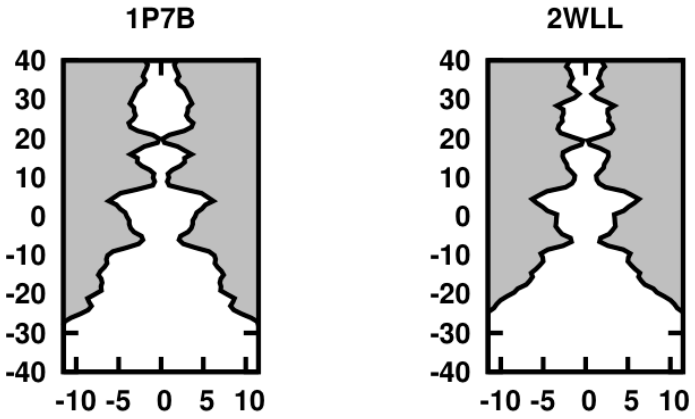

Figure S2. Calculated pore radius profiles for KirBac1.1 pdb structures. The pore axis is vertical, and the radius is horizontal, both are in Å. The G-loop is positioned at 0 Å, with the transmembrane domain > 0 Å and cytoplasmic domain < 0 Å. The pdb codes are labeled above each plot. Radii are calculated according to previously described methods (10).

FIG. S3

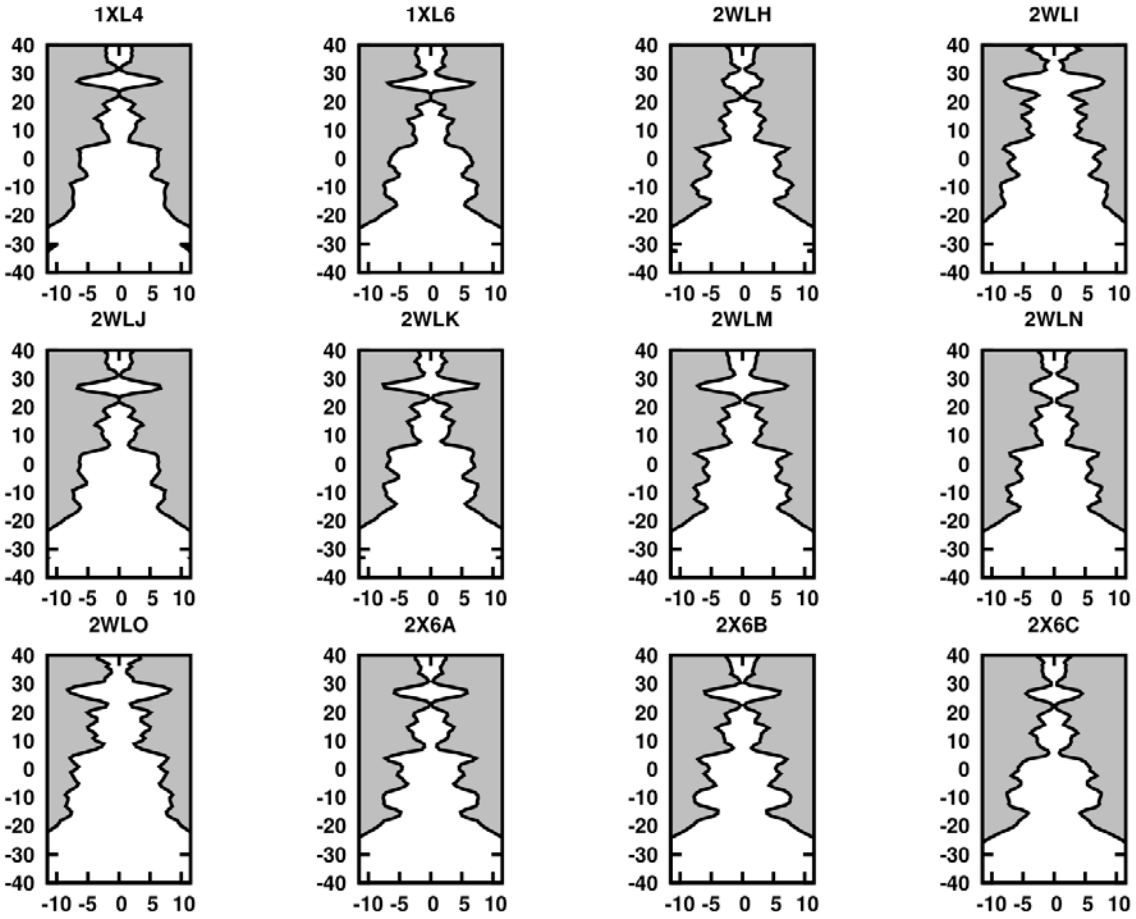

Figure S3. Calculated pore radius profiles for KirBac3.1 pdb structures. The pore axis is vertical, and the radius is horizontal, both are in Å. The G-loop is positioned at 0 Å, with the transmembrane domain > 0 Å and cytoplasmic domain < 0 Å. The pdb codes are labeled above each plot. Radii are calculated according to previously described methods (10).

FIG. S4

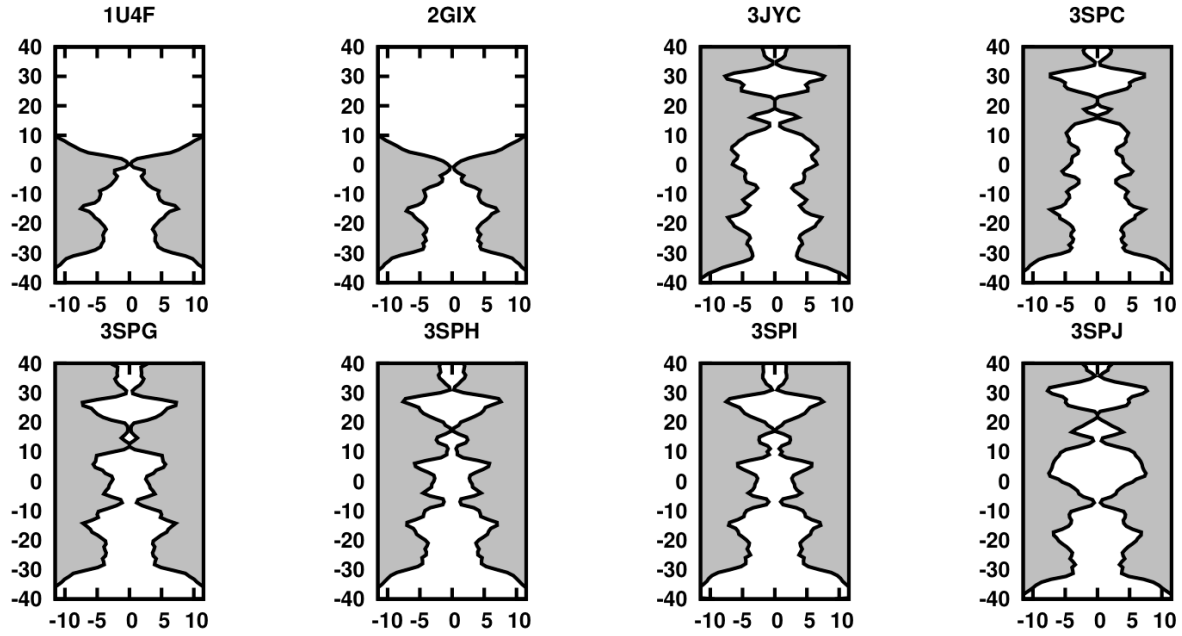

Figure S4. Calculated pore radius profiles for Kir2.x pdb structures. The pore axis is vertical, and the radius is horizontal, both are in Å. The G-loop is positioned at 0 Å, with the transmembrane domain > 0 Å and cytoplasmic domain < 0 Å. The pdb codes are labeled above each plot. Radii are calculated according to previously described methods (10).

FIG. S5

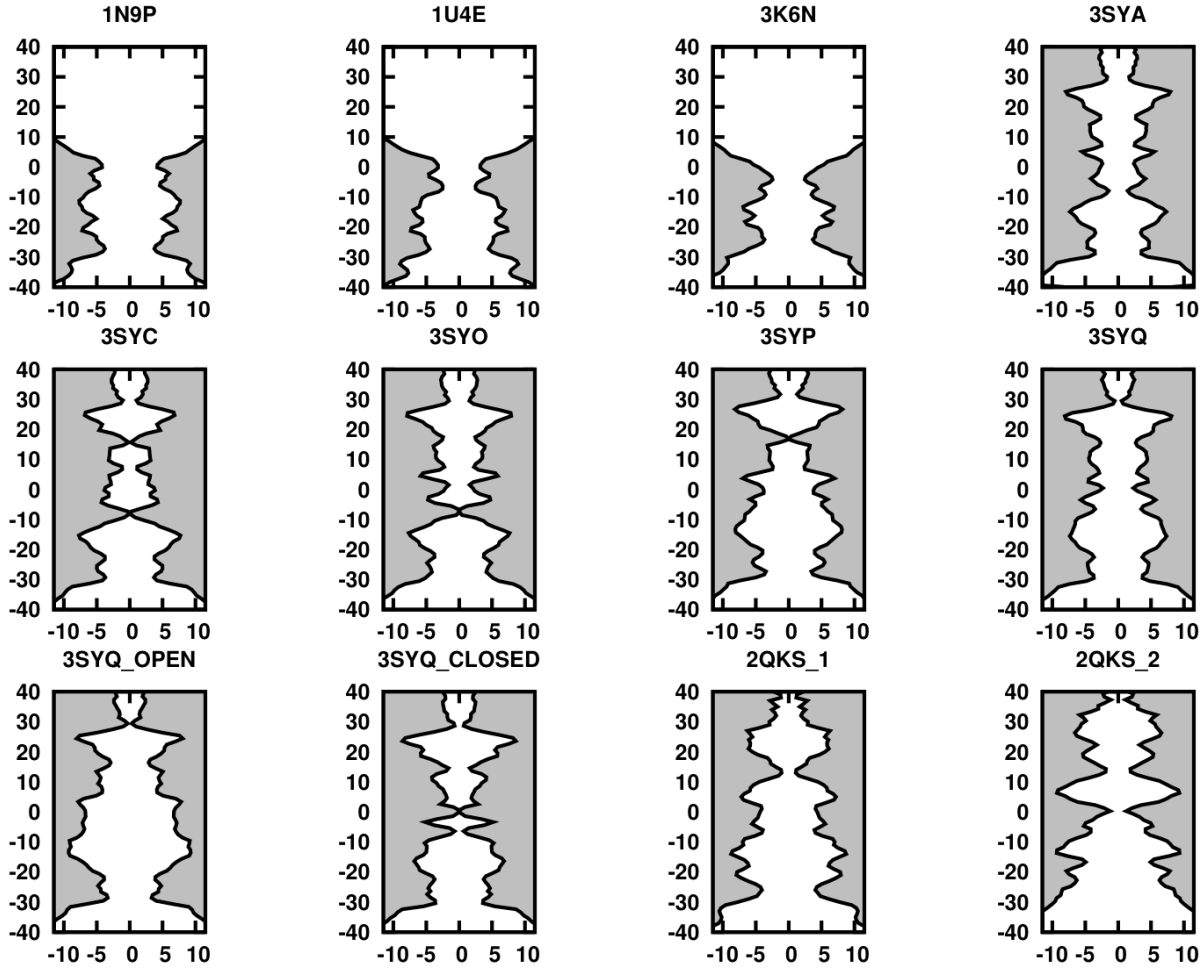

Figure S5. Calculated pore radius profiles for Kir3.x pdb structures. The pore axis is vertical, and the radius is horizontal, both are in Å. The G-loop is positioned at 0 Å, with the transmembrane domain > 0 Å and cytoplasmic domain < 0 Å. The pdb codes are labeled above each plot. Pdb 2QKS is of a KirBac-Kir3.1 chimera. Radii are calculated according to previously described methods (10).

FIG. S6

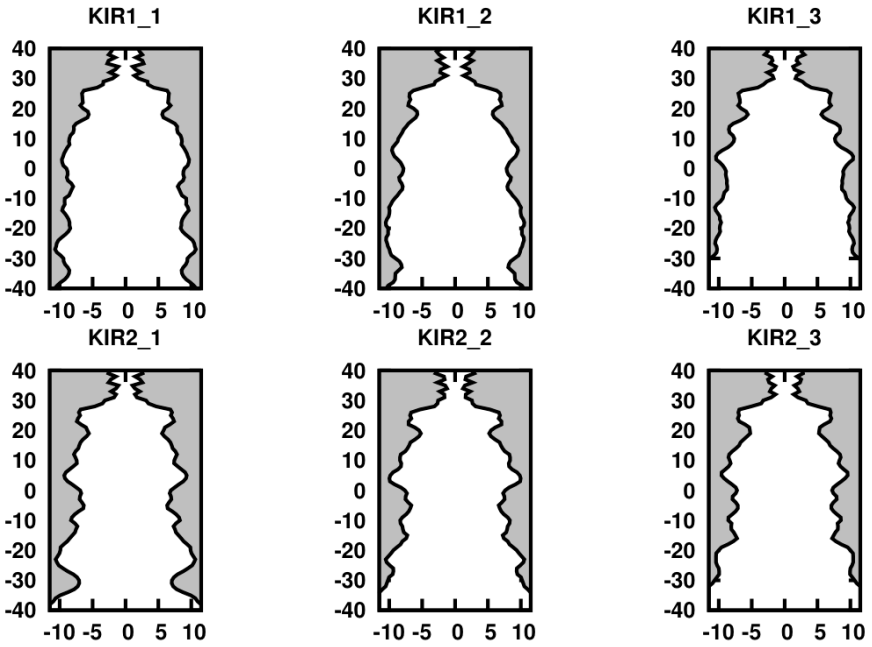

Figure S6. Calculated pore radius profiles for models of Kir1.1 and Kir2.1 based on the open model of KirBac1.1. The pore axis is vertical, and the radius is horizontal, both are in Å. The G-loop is positioned at 0 Å, with the transmembrane domain > 0 Å and cytoplasmic domain < 0 Å. Three separate models were generated based on different starting sequence alignments for each channel type. Radii are calculated according to previously described methods (10).

FIG. S7

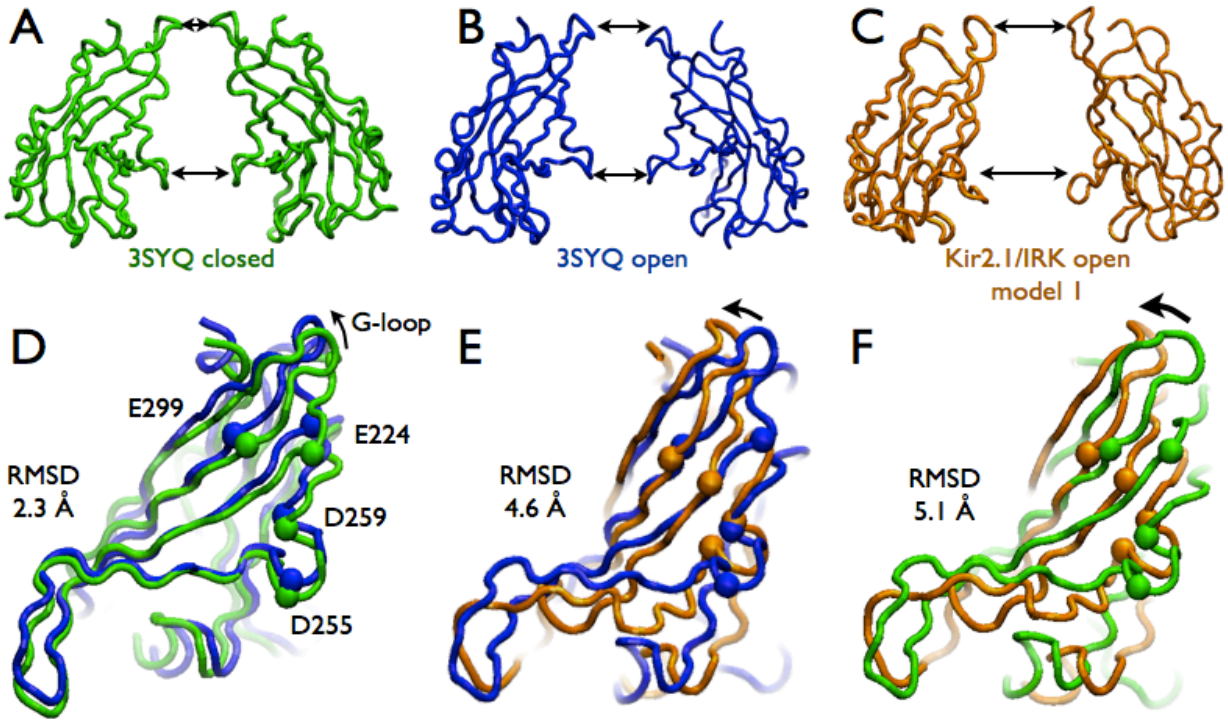

Figure S7. Comparison of Kir2.1/IRK homology model with the x-ray crystal structure of Kir3.2/GIRK in multiple conformations. X-ray structure of Kir3.2/GIRK2, pdb code 3SYQ, with opposing subunits of the cytoplasmic domain in different conformations(9). In the same crystal structure, they found two cytoplasmic subunits in the (A) closed state and two subunits bound to PIP_2 giving an open or partially open state (B). (C) A homology models of an open Kir2.1/IRK used in this study. The two subunits of the different structures are C_α RMSD aligned onto one another, including the conformational change in the RMSD. (D) GIRK2-open (blue) on GIRK2-closed (green), with a RMSD of 2.3 Å. The C_α atoms for residues corresponding to E224, D255, D259 and E299 in Kir2.1/IRK, are shown as spheres in each of the models. The G-loop upper gate is labeled. (E) Kir2.1/IRK-open (orange) onto GIRK2-open (blue) with RMSD of 4.6 Å. (F) Kir2.1/IRK-open (orange) onto GIRK2-closed (green) with RMSD 5.1 Å.

FIG. S8

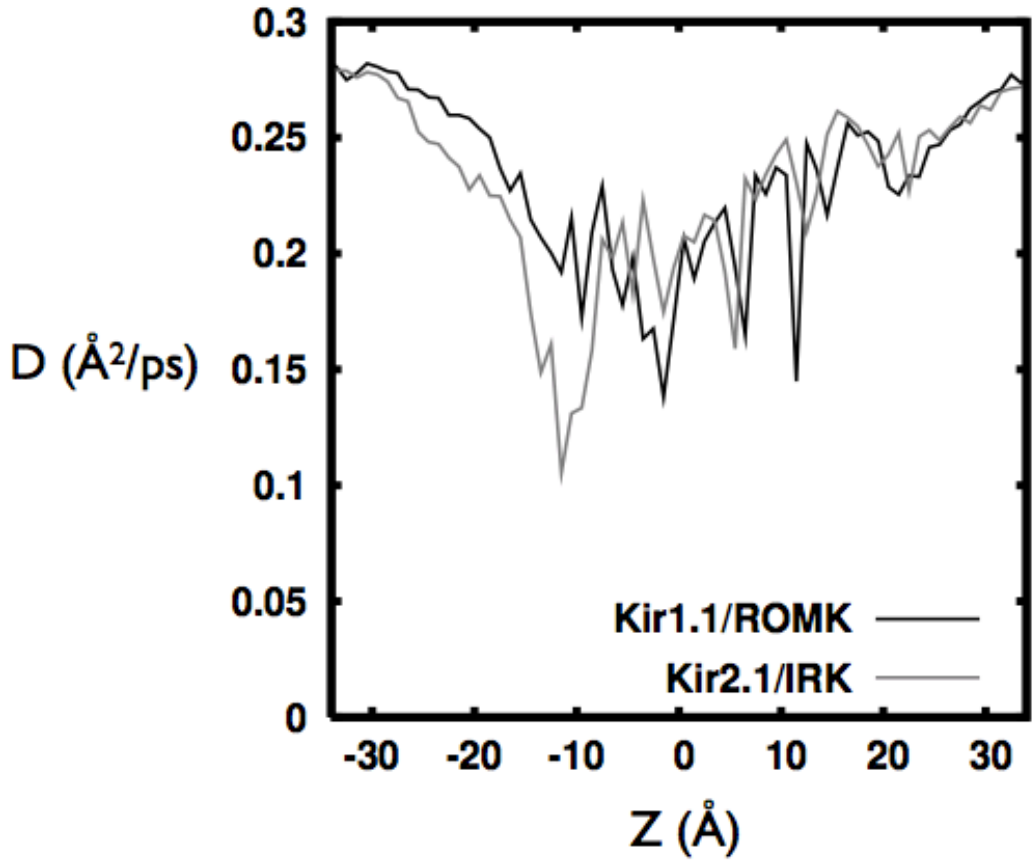

Figure S8. **Calculated diffusion constant of K^+ inside the cytoplasmic pore of Kir1.1/ROMK and Kir2.1/IRK**. To determine the diffusion constant profile, trajectory data was filtered to select only data where the ion resides inside the cytoplasmic pore defined from -35 Å < Z < 35 Å and R < 20 Å. Then, for each Z position, the diffusion constant was calculated using the equation $D = \langle[\Delta Z(t)-\langle\Delta Z(t)\rangle]^2\rangle/2\tau$, where $\Delta Z(t) = Z(t+\tau)-Z(t)$ and τ = 1 ps (11). The profiles demonstrate a decrease in ion diffusion inside the cytoplasmic pore. The experimental diffusion constant of K^+ is 0.185 $Å^2$/ps (12), however it is well documented that the diffusion of K^+ in these simulations is over-estimated because the TIP3 water model itself produces a diffusion constant twice that of experimental values (13, 14). The bulk values in these calculations correspond to other molecular dynamics simulations at 1 M KCl at comparable temperatures (11). Note that a diffusion constant of 0.1 $Å^2$/ps corresponds to 10^{-5} cm^2/s.

FIG. S9

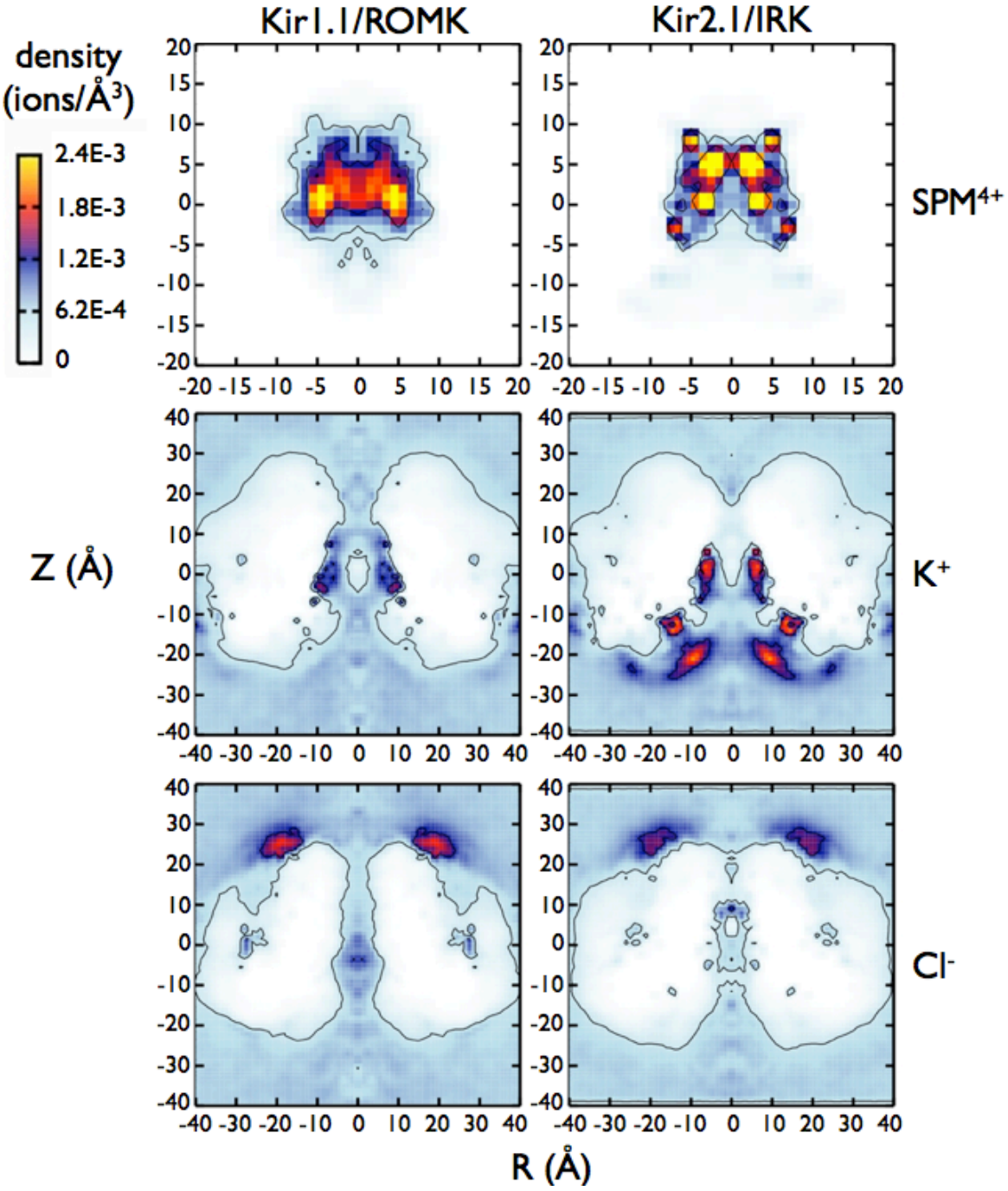

Figure S9. Average SPM^{4+}, K^+ and Cl^- density distributions. The density for spermine is calculated using the four nitrogen atoms (N_1, N_2, N_3, N_4). A molecular density of $\rho = 6.022 \times 10^{-4}$ ions/Å^3 corresponds to 1 M concentration. Contours are shown for densities corresponding to 1 and 2.5 M. Note that while K^+ and Cl^- adequately sample the system space and converge to 1 M in the bulk, the SPM^{4+} molecule remains mostly in the pore throughout the simulations.

SUPPLEMENTARY REFERENCES

1. Nishida M, MacKinnon R. 2002. Structural basis of inward rectification: cytoplasmic pore of the G protein-gated inward rectifier GIRK1 at 1.8 A resolution. *Cell* 111: 957-65
2. Kuo A, Gulbis JM, Antcliff JF, Rahman T, Lowe ED, et al. 2003. Crystal structure of the potassium channel KirBac1.1 in the closed state. *Science* 300: 1922-6
3. Pegan S, Arrabit C, Zhou W, Kwiatkowski W, Collins A, et al. 2005. Cytoplasmic domain structures of Kir2.1 and Kir3.1 show sites for modulating gating and rectification. *Nat Neurosci* 8: 279-87
4. Clarke OB, Caputo AT, Hill AP, Vandenberg JI, Smith BJ, Gulbis JM. 2010. Domain reorientation and rotation of an intracellular assembly regulate conduction in Kir potassium channels. *Cell* 141: 1018-29
5. Nishida M, Cadene M, Chait BT, MacKinnon R. 2007. Crystal structure of a Kir3.1-prokaryotic Kir channel chimera. *Embo J* 26: 4005-15
6. Tao X, Avalos JL, Chen J, MacKinnon R. 2009. Crystal structure of the eukaryotic strong inward-rectifier K+ channel Kir2.2 at 3.1 A resolution. *Science* 326: 1668-74
7. Xu Y, Shin HG, Szep S, Lu Z. 2009. Physical determinants of strong voltage sensitivity of K(+) channel block. *Nat Struct Mol Biol* 16: 1252-8
8. Hansen SB, Tao X, MacKinnon R. Structural basis of PIP2 activation of the classical inward rectifier K+ channel Kir2.2. *Nature* 477: 495-8
9. Whorton MR, MacKinnon R. Crystal structure of the mammalian GIRK2 K+ channel and gating regulation by G proteins, PIP2, and sodium. *Cell* 147: 199-208
10. Jogini V, Roux B. 2005. Electrostatics of the intracellular vestibule of K+ channels. *J Mol Biol* 354: 272-88
11. Im W, Roux B. 2002. Ions and counterions in a biological channel: a molecular dynamics simulation of OmpF porin from Escherichia coli in an explicit membrane with 1 M KCl aqueous salt solution. *J Mol Biol* 319: 1177-97
12. Mills R and Lobo VM. 1989. Self-Diffusion in Electrolyte Solutions—A Critical Examination of Data Compiled from the Literature, Elsevier, Amsterdam.
13. van der Spoel D, van Maaren PJ and Berendsen HJC. 1998. A systematic study of water models for molecular simulation: Derivation of water models optimized for use with a reaction field. J Chem Phys 108 pp. 10220-10230.
14. Mahoney WW and Jorgensen WL. 2001. Diffusion constant of the TIP5P model of liquid water. J. Chem. Phys., 114, 363-366.